6170–6182 *Nucleic Acids Research, 2006, Vol. 34, No. 21* *Published online 6 November 2006*
doi:10.1093/nar/gkl840

PARP-1 and Ku compete for repair of DNA double strand breaks by distinct NHEJ pathways

Minli Wang, Weizhong Wu, Wenqi Wu, Bustanur Rosidi, Lihua Zhang, Huichen Wang[1] and George Iliakis*

University of Duisburg-Essen, Medical School, Institute of Medical Radiation Biology, Hufeland street 55, 45122 Essen, Germany and [1]Center for Neurovirology, Temple University, 1900 North 12th, Philadelphia, PA 19122, USA

Received August 31, 2006; Revised October 3, 2006; Accepted October 8, 2006

ABSTRACT

Poly(ADP-ribose)polymerase 1 (PARP-1) recognizes DNA strand interruptions *in vivo* and triggers its own modification as well as that of other proteins by the sequential addition of ADP-ribose to form polymers. This modification causes a release of PARP-1 from DNA ends and initiates a variety of responses including DNA repair. While PARP-1 has been firmly implicated in base excision and single strand break repair, its role in the repair of DNA double strand breaks (DSBs) remains unclear. Here, we show that PARP-1, probably together with DNA ligase III, operates in an alternative pathway of non-homologous end joining (NHEJ) that functions as backup to the classical pathway of NHEJ that utilizes DNA-PKcs, Ku, DNA ligase IV, XRCC4, XLF/Cernunnos and Artemis. PARP-1 binds to DNA ends in direct competition with Ku. However, in irradiated cells the higher affinity of Ku for DSBs and an excessive number of other forms of competing DNA lesions limit its contribution to DSB repair. When essential components of the classical pathway of NHEJ are absent, PARP-1 is recruited for DSB repair, particularly in the absence of Ku and non-DSB lesions. This form of DSB repair is sensitive to PARP-1 inhibitors. The results define the function of PARP-1 in DSB repair and characterize a candidate pathway responsible for joining errors causing genomic instability and cancer.

INTRODUCTION

Endogenous cellular processes and exogenous factors, such as ionizing radiation (IR) generate highly cytotoxic double strand breaks (DSBs) in the DNA that undermine genomic integrity. Higher eukaryotes utilize a pathway of non-homologous end joining (NHEJ) to repair the majority of DSBs that employs the products of *DNA-PKcs*, *KU70*, *KU80*, *LIG4*, *XRCC4* and *Artemis* (1,2), as well as the recently characterized factor *XLF*/*Cernunos* (3,4). Proteins of this pathway are important caretakers of the mammalian genome and knock out of *KU*, *LIG4*, or *XRCC4* invariably leads to cancer on a $p53^{-/-}$ background (5–7).

Tumors formed in the above mutant mice, mainly pro-B lymphomas, carry chromosomal translocations linking an amplified c-myc oncogene with the IgH locus sequences. The initial non-reciprocal translocation event, as well as the subsequent steps in the amplification process requires joining of DNA ends. Due to the defect in the DNA-PK dependent pathway (D-NHEJ), end joining must be carried out in these mutants by an alternative process prone to missjoining and possibly utilizing microhomologies (8–10). Alternative pathways of end joining are also implicated in genomic instability (5,11,12), in the formation of soft tissue sarcomas (13) and in the aberrant coding and signal joints formed during V(D)J recombination (14–17) in NHEJ mutant mice.

Furthermore, alternative forms of end joining operate in the repair of IR-induced DSBs. Mutants with defects in NHEJ show pronounced inhibition but still rejoin the majority of DSBs by a slowly operating pathway (18–20). Because this repair pathway does not show dependence on genes of HRR (20), it is thought to reflect an alternative form of end joining that functions as backup (B-NHEJ) to the DNA-PK dependent pathway (D-NHEJ).

These results implicate alternative pathways of end joining in genomic integrity through contributions to DSB repair, particularly when D-NHEJ is compromised. However, due to their low fidelity, the same repair pathways are directly implicated in genomic instability and cancer. Despite the potentially grave consequences of their functions, little is known about the biochemistry of these pathways, as well as the mechanisms of their regulation and integration into the

*To whom correspondence should be addressed. Tel: +49 201 723 4152; Fax: +49 201 723 5966; Email: Georg.Iliakis@uk-essen.de
Present address:
Weizhong Wu, Liver Cancer Institute and Zhongshan Hospital, Fudan University, 136 Yi Xue Yuan Road, Shanghai 200032, P.R.China

The authors wish it to be known that, in their opinion the first two authors should be regarded as joint First Authors

cellular DNA DSB processing machinery, beyond the observation that they frequently utilize microhomologies (8,9).

Recent work identifies DNA ligase III as a candidate factor in alternative pathways of NHEJ (21,22) and points to PARP-1 as an additional potential contributor (22). PARP-1 is an abundant nuclear enzyme of higher eukaryotes that has been implicated in many cellular processes including DNA repair. It is a member of a superfamily of eighteen proteins containing PARP domains, of which only PARP-2 has also been implicated in DNA damage response (23–25). The 116 kDa PARP-1 has two zinc finger motifs that mediate binding to single strand breaks (SSBs) and DSBs. This binding enables the protein to cleave NAD^+ to nicotinamide and ADP-ribose and to form branched ADP-ribose polymers on glutamic acid residues of target proteins, including itself.

PARP-1 is involved in SSB repair, BER or NER, together with XRCC1, DNA ligase III, as well as polynucleotide kinase (PNK), PCNA and FEN1 (26,27) and plays an essential role in removing lesions converted to DSBs during DNA replication (28,29). Although PARP-1 is implicated in DSB repair (30–33) the results are variable and the mechanism unknown (23,34,35). Here, we present experiments demonstrating that PARP-1 contributes to DSB repair as a component of an alternative pathway of NHEJ.

MATERIALS AND METHODS

Cell culture, chemicals and irradiation

The cell lines M059J and M059K (36), were grown in DMEM supplemented with 10% fetal calf serum (FCS), 1% non-essential amino acids and 1% L-glutamine. $Ku70^{-/-}$ (37) cells were maintained in MEM and *LIG4*$^{-/-}$ (6), MEFs were maintained in D-MEM plus 10% FCS. COM3, COR3 and COC1 cells are derivatives of the SV40 transformed Chinese hamster cell line, CO60 (30). COM3 cells express PARP-1 DBD under the control of the mouse mammary tumor virus long terminal repeat sequence that confers dexamethasone (Dex) inducibility. COR3 is a control cell line generated by transfection of CO60 cells with the HGO and pTKhygro expression constructs. COC1 is a cell line constitutively overexpressing the PARP-1 DBD. All CO60 derivatives were maintained in DMEM containing 5% FCS. When necessary, geneticin (800 μg/ml) and/or hygromycin (800 U/ml) were added, but were generally removed 24 h before inception of the experiment. xrs-6 is a CHO mutant with a defect in *KU80* and *xrs-6*/*KU80* a cell line generated by transfecting with the human *KU80* under the control of the Rous sarcoma virus long terminal repeat promoter (38). V3 is a DNA-PKcs deficient CHO cell line. Cells were cultured in McCoy's 5A medium supplemented with 5% FCS.

3′-Aminobenzamide (3′-AB) (Sigma) was dissolved in dimethyl sulfoxide (DMSO) (4 M) and used at 10 mM. 3,4-Dihydro-5-[4-(1-piperidinyl)butoxy]-1(2*H*)-isoquinolinone (DPQ) (Alexis Biochemicals) was dissolved in DMSO (16.8 mM) and used at 10 μM. 1,5-Dihydroxyisoquinoline (DIQ) (Sigma) was dissolved in DMSO (0.5M) and used at 100 μM. Wortmannin (Wort) (Sigma) was dissolved in DMSO (25 mM) and used at 20 μM. Cells were exposed to X-rays using a Pantak X-ray machine operated at 320 kV, 10 mA with a 1.6 mm Al filter (effective photon energy about 90 kV), at a dose rate of 2.7 Gy/min.

Western blotting and immunofluorescence

Western blotting was used to detect PARP-1 and PARP-1 DBD expression, as well as pADPr. For this purpose nuclear, cytoplasmic or whole cell extracts were prepared using standard procedures. After electrophoresis in 10% SDS–PAGE and electroblotting (PVDF membrane, Millipore, Germany), the membrane was processed according to the instructions of the manufacturer (Amersham Biosciences). PARP-1 and PARP-1 DBD were visualized with a rabbit anti-PARP-1 antibody (Calbiochem). pADPr was detected with rabbit anti-pADPr antibody (Calbiochem). Intracellular NAD^+ levels were determined in irradiated and non-irradiated cells using an enzymatic cycling assay (39,40). For indirect immunofluorescence, cells grown on poly-L-lysine treated coverslips were permeabilized with 10 mM HEPES (pH 7.4), 300 mM Sucrose, 100 mM NaCl, 3 mM $MgCl_2$, freshly added protease inhibitor cocktail (Boehringer) and 0.5% Triton X-100 and were subsequently incubated with 10% TCA (20 min, RT) and then with 0.5% Nonidet P40 (5 min). Slides were blocked for 1 h at room temperature with 10% FCS in phosphate-buffered saline (PBS) and incubated with 1:100 diluted rabbit anti-(ADP-ribose)-polymer IgG (Calbiochem) followed by Alexa Fluor 488 or fluorescein isothiocyanate (FITC) conjugated goat anti-rabbit IgG (1:500, Molecular Probes). Immunofluorescence was evaluated with a confocal laser scanning microscope (TCS4, Leica, Germany). A mouse monoclonal antibody against Ku70, clone N3H10 and Ku80, clone 111, were from Kamiya Biomedical Co. (Seattle, WA); a mouse monoclonal antibody against GAPDH, from Chemico International. Semi-purified PARP-1 (specific activity: 261 nmol ADP-ribose/min/mg total protein at 25°C) was from Biomol (Hamburg). Ku was purified from baculovirus infected Sf9 cells as described previously (41).

Pulsed-field gel electrophoresis (PFGE)

Asymmetric Field Inversion Gel Electrophoresis (AFIGE) was used for the quantification of DNA DSBs after exposure to IR, as described previously (19,42). Cells were embedded in agarose (InCert agarose, BioRad) and processed for lysis. In divergence to the original protocol and in order to reduce conversion of heat labile sites to DSBs (43), high temperature was avoided during lysis. Agarose blocks were lysed in a buffer (pH 8.0) containing 400 mM EDTA, 2% NLS, 0.3 mg/ml proteinase K at 4°C for 16 h; they were subsequently washed with TE buffer and incubated for 24 h at 4°C in a solution containing 1.85 M NaCl, 0.15 M KCl, 4 mM Tris, 0.5% Triton X-100 (pH 7.5). PFGE was carried out, after RNAase treatment, in 0.5% agarose gels cast in the presence of ethidium bromide, in 0.5× TBE at 8°C for 40 h using alternating cycles of 50 V (1.25 V/cm) for 900 s in the forward direction and 200 V (5.0 V/cm) for 75 s in the reverse direction. Gels were scanned in the Typhoon and analyzed using the ImageQuant software (GE Biosciences). The fraction of DNA released (FDR) from the well into the lane is a measure of DSBs present. FDR measured in non-irradiated samples

(background; usually between 2–8%) was subtracted from FDR measured in samples exposed to IR.

In vivo plasmid end joining

To document a role for PARP-1 in DNA end joining *in vivo* we employed a fast-readout plasmid rejoining assay utilizing the plasmid pEGFP-Pem1-Ad2 (44). The plasmid was digested with HindIII, or I-SceI, to remove Ad2 and generate different types of ends. Supercoiled pEGFP-Pem1 was used as a positive control to standardize the transfection and analysis conditions. The pDsRed2-N1 plasmid (Clontech) was co-transfected with either linearized pEGFP-Pem1-Ad2 or supercoiled pEGFP-Pem1 as a control of transfection efficiency. Plasmids were transfected using the MEF1 nucleofector kit in the Nucleofector devise (Amaxa) according to the instructions of the manufacturer. Green (EGFP) and Red (DsRed) fluorescence were measured by flow cytometry 24 h later (21). The EGFP signal in this assay increases initially, approximately linearly, with increasing amount of plasmid, but reaches at higher concentrations a plateau in a cell-line-dependent manner (44). To avoid measurements near the plateau region that compromise quantification, calibration curves were generated for each cell lines using circular pEGFP-Pem1 plasmid (M. Wang and G. Iliakis, unpublished data). The results were used to select cell-line-dependent amounts of linear pEGFP-Pem1-Ad2 plasmid allowing evaluation of the effects of PARP-1 inhibitors in each cell line. However, since different cell lines have different calibration curves and because the results obtained have not been normalized against a common standard, the signal levels shown cannot be taken as a direct measure of the DNA end joining capacity of each cell line—i.e. they do not directly reflect the absolute end joining levels of each cell line.

For cell cycle analysis, cells were trypsinized and fixed in 70% ethanol. They were stained in PBS containing 62 μg/ml RNase A and 40 μg/ml propidium iodide at 37°C for 15 min.

RNA interference

RNA interference, mediated by siRNAs was used to knock-down *Ku* expression in *LIG4*$^{-/-}$ MEFs. For this purpose the sequences S1: GGAUCAUGCUGUUCACCAA (487 nt downstream), as well as the unique negative control duplex (OR-0030-neg05) were synthesized (Eurogentec, Belgium) and tested by transfection with electroporation under the conditions described above using 5×10^6 cells and 10 μg *KU* or control siRNA per transfection reaction. After transfection, cells were returned to normal growth conditions and the level of knock-down evaluated by western blotting. To test the effect of Ku knock-down on DNA DSB repair, siRNA treated cells were transfected with test and control plasmids and rejoining efficiency measured 24 h later.

Electrophoretic mobility shift assay (EMSA)

Competition between Ku and PARP-1 for DNA end binding was assessed by EMSA (45,46). Oligonucleotides used were OA (G-GCC-GCA-CGC-GTC-CAC-CAT-GGG-GTA-CAA), OB (G-TAG-TTG-TAC-CCC-ATG-GTG-GAC-GCG-TGC), OB1 (T-TGT-ACC-CCA-TGG-TGG-ACG-CGT-GCG-GCC) and OB3 (T-GTA-CCC-CAT-GGT-GGA-CGC-GTG-CGG-CCT). Annealing of OA with OB, OB1 or OB3 resulted in double-stranded DNA molecules with 4 nt overhang, blunt ends and one nucleotide overhang at 3′ ends, respectively. They were 3′ end labeled with ^{32}P using [γ-^{32}P]ATP and polynucleotide kinase (Fermentas). End binding was assessed by incubating 1 ng (unless stated otherwise) of ^{32}P labeled DNA with protein in a buffer containing 10 mM Tris–HCl (pH 7.5), 1 mM EDTA, 0.5% glycerol, 1 mM DTT and 150 mM NaCl at 25°C for 20 min. Supershift of the Ku band was achieved with an anti-Ku80 antibody (Kamiya, Clone 111) added to the reaction before the substrate DNA. Reactions were electrophoresed on a 6% polyacrylamide gel in 0.5× TBE buffer. The gels were dried and analyzed in the Typhoon (GE Biosciences).

RESULTS

PARP-1 inhibition compromises rejoining of DNA DSBs in the absence of Ku

Although PARP-1 has been repeatedly implicated in the repair of DNA DSBs, a consistent model explaining existing data and placing this enzyme in a network with other known DSB repair pathways is not available. The genetic and biochemical implication of DNA Ligase III, with which PARP-1 frequently cooperates, in backup pathways of end joining (see Introduction) offer alternative ways of interpretation for existing data and a rationale for the formulation of alternative hypotheses. We reasoned that if PARP-1 is involved in backup pathways of NHEJ, a way for documenting this contribution would be by applying PARP-1 inhibitors to D-NHEJ deficient mutants or by combining PARP-1 with DNA–PK inhibitors.

In the repair proficient human glioma M059K cells, 3′-aminobenzamide (3′-AB) has no detectable effect on DSB repair (Supplementary Figure 1B and C), although immunofluorescence of poly(ADP-ribose) shows that PARP-1 activity is significantly reduced (Supplementary Figure 1A). We reasoned that if PARP-1 is involved in alternative pathways of NHEJ, exposure of D-NHEJ deficient mutants to PARP-1 inhibitors should uncover this contribution. Therefore, the same experiment was carried out in M059J cells that lack DNA–PK activity due to a frameshift mutation in *DNA–PKcs* (36,47). M059J cells show reduced efficiency for DSB rejoining after IR (19,36), as compared to M059K cells, but repair nevertheless the majority of DSBs with slow kinetics via DNA–PK independent mechanisms (19). Despite the defect in D-NHEJ, treatment with 3′-AB fails to inhibit DSB rejoining (Supplementary Figure 1B and C); similar results are obtained with DPQ, another widely used PARP-1 inhibitor (data not shown).

Ligation is the final step in DNA end joining and D-NHEJ recruits DNA ligase IV in this function. Compared to wild-type cells, *LIG4*$^{-/-}$ cells have significantly reduced rejoining efficiency but remove over 70% of DSBs with slower kinetics through a DNA ligase IV-independent pathway (Figure 1A). Treatment with 3′-AB has no effect on wild-type cells, but exerts a small effect on *LIG4*$^{-/-}$ cells.

A prerequisite for PARP-1 activation and therefore involvement in DSB repair is binding to DNA ends. In the above mutants and despite the defects in DNA–PKcs and DNA ligase IV, Ku is present at normal intracellular levels

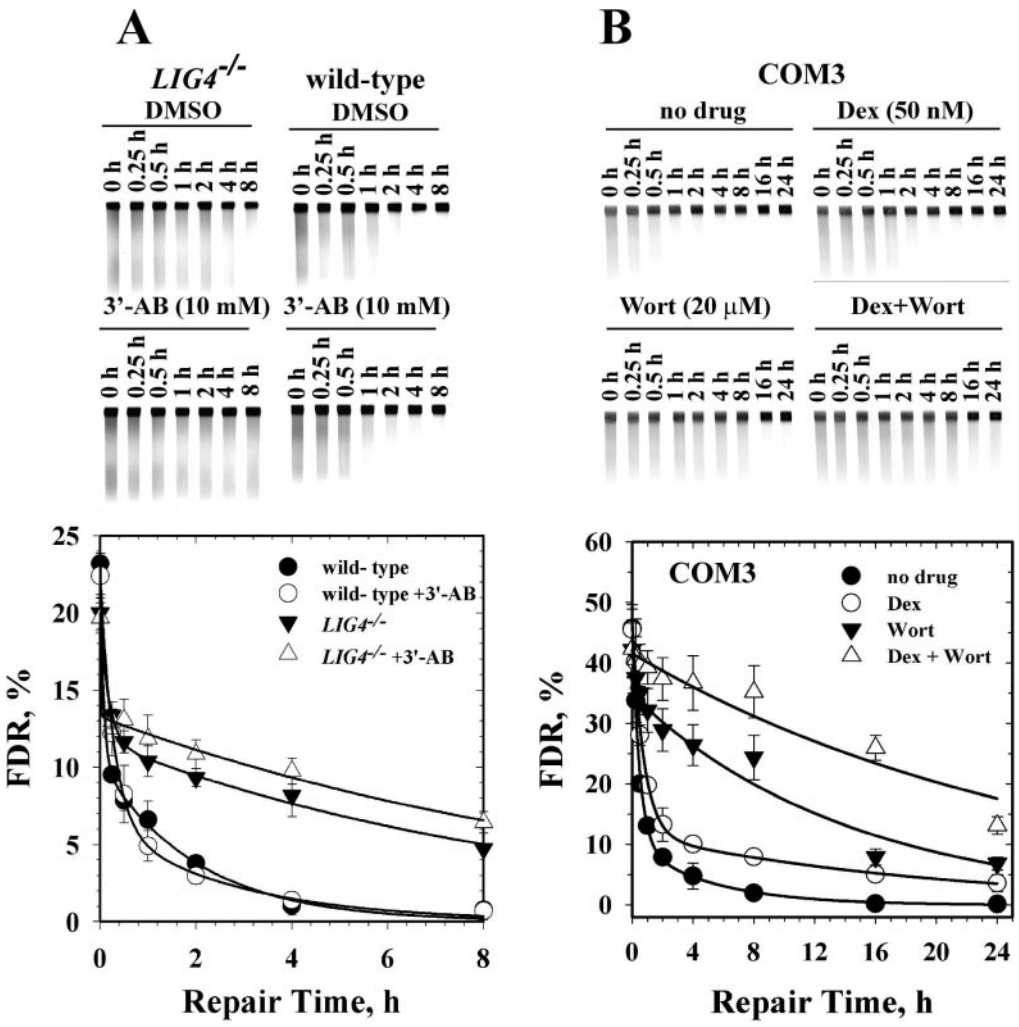

Figure 1. Effect on DNA DSB rejoining of PARP-1 inhibitors in LIG4$^{-/-}$ MEFs, as well as of PARP-1 DBD expression in Chinese hamster cells after exposure to IR. (**A**) p53$^{-/-}$/LIG4$^{-/-}$ and p53$^{-/-}$ MEFs (wild-type) were pretreated with 10 mM 3′-AB or solvent (DMSO <0.4% v/v in medium) for 1 h, exposed to 30 Gy X-rays and returned to 37°C for repair. At various times thereafter cells were collected and prepared for AFIGE to measure residual DNA DSBs. The upper panel shows gels from a typical experiment and the lower panel the results of their quantitative analysis. Plotted is FDR, a measure of DNA DSBs present, as a function of the repair time. Shown are the means and standard errors calculated from four determinations in two experiments. The value of FDR measured in non-irradiated cells has been subtracted from the results shown. Standard lysis conditions were used in these experiments but similar results have been obtained with low temperature lysis. (**B**) COM3 cells expressing the PARP-1 DBD under the control of the mouse mammary virus LTR that is dexamethasone inducible were incubated with 50 nM dexamethasone for 24 h or left untreated. Thereafter, cells were exposed to 40 Gy and allowed to repair at 37°C in the presence (20 μM) or absence of wortmannin (given 1 h before IR). Repair of DSBs was measured by AFIGE and is expressed as FDR versus repair time. The upper panel shows typical gels and the lower panel the repair kinetics plotted as FDR versus time. Shown are the means and standard errors calculated from six determinations in three experiments.

(46). We reasoned that in the absence of key D-NHEJ components, Ku will bind DNA ends non-productively and will exert a dominant negative effect that will limit the engagement of PARP-1. To examine this possibility, we tested a radiation sensitive Chinese hamster mutant, xrs-6, defective in Ku80 as a result of a nonsense mutation, and a corrected clone, xrs-6/Ku80, derived by ectopic expression of human *Ku80* (38) (Figure 2A and B). Ku80 deficiency compromises DSB rejoining in xrs-6 cells as compared to xrs-6/Ku80, but here again alternative pathways remove over 80% of DSBs within 24 h (Figure 2B). While DPQ has no detectable effect on DSB rejoining in corrected cells, it produces a clear inhibition in xrs-6 cells. The greater inhibition of DSB repair is not caused by a greater inhibition of PARP-1 in *Ku80* deficient cells, as similar inhibition is observed for both types of cells (Figure 2A). Despite slight differences in response, DPQ is also effective in inhibiting DSB rejoining in fibroblasts derived from *Ku70*$^{-/-}$ mice (37) (Figure 2C). This result suggests that the observed phenotype is not a peculiarity of Ku80 deficient Chinese hamster cells, but can also be observed in *Ku70*$^{-/-}$ MEFs. Thus, in agreement with competition against Ku, the contribution of PARP-1 to alternative pathways of NHEJ is clearly detectable in Ku deficient, very small in *LIG4*$^{-/-}$ and undetectable in DNA–PKcs deficient cells.

Overexpression of PARP-1 DBD inhibits rejoining of DNA DSBs

Overexpression of the PARP-1 DNA-binding domain (DBD) causes a trans-dominant inhibition of poly(ADP-ribosyl)ation

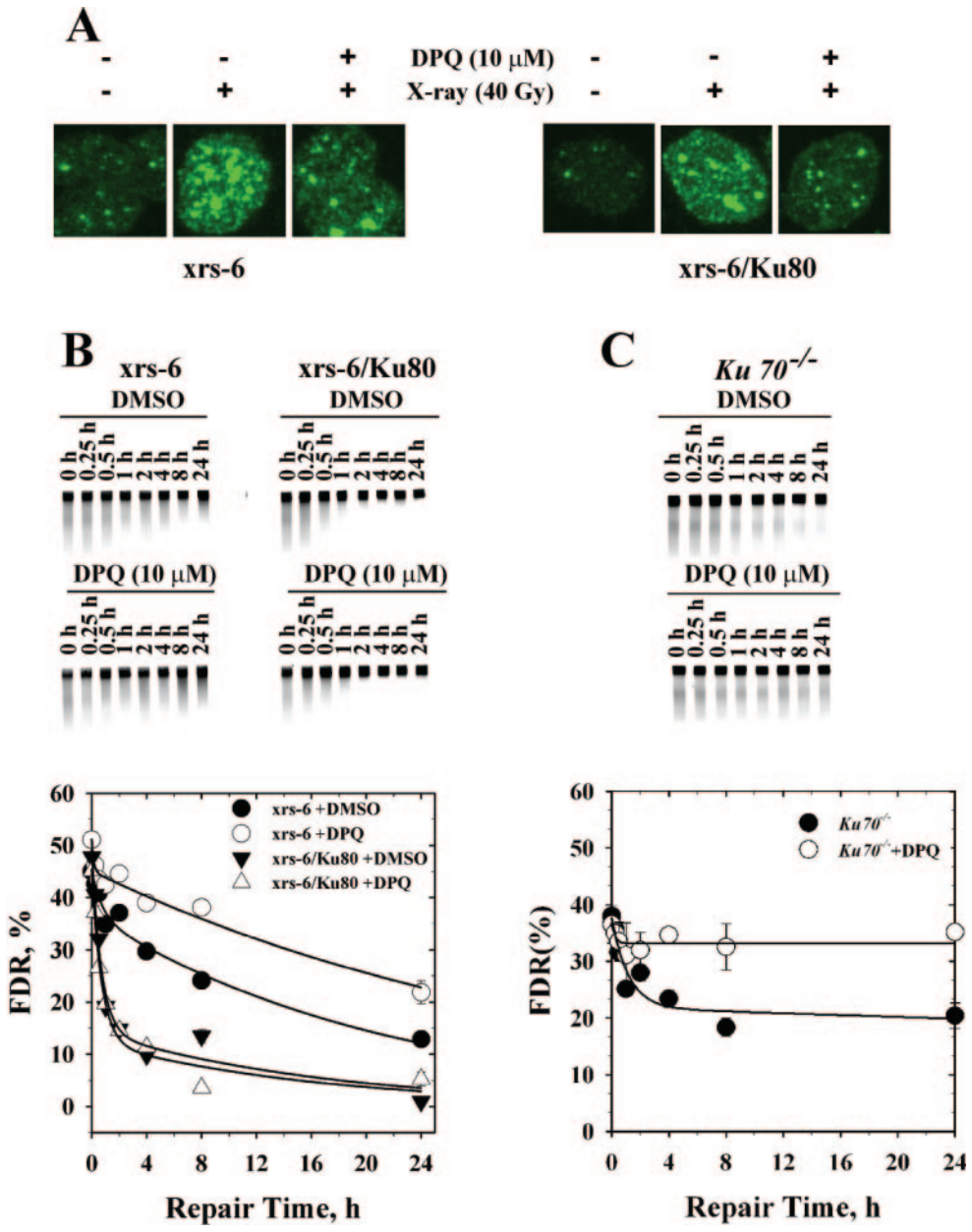

Figure 2. Effect of PARP-1 inhibitors on Ku deficient cells. (**A**) The effect of DPQ (10 μM), or DMSO on poly(ADP-ribose) levels in *Ku80* deficient *xrs-6* cells, as well as in their corrected counterpart *xrs-6*/*KU80* cells. Cells growing on coverslips were exposed to 40 Gy X-rays and prepared for immunofluorescence 15 min later. The poly(ADP-ribose)-associated fluorescence in non-irradiated, irradiated, as well as irradiated and treated cells is shown for xrs-6 and xrs-6/Ku80 cells, respectively. DPQ inhibits PARP-1 activity in both cell lines. (**B**) Rejoining of IR-induced DNA DSBs in xrs-6 cells and xrs-6/Ku80 cells in the presence or absence fo DPQ (10 μM). Results from four determinations in two experiments are shown. Other details as in Figure 1. (**C**) DNA DSB repair kinetics in *Ku70* deficient cells after treatment with DPQ. Results from two determinations in one experiment are shown. Other details as in Figure 1.

interrupting several functions of PARP-1 (30,48). Because the PARP-1 DBD can in principle also bind to DNA ends and compete with Ku, we wished to evaluate the effect of its expression on the rejoining of IR-induced DNA DSBs. We introduced this approach, first because high levels of PARP-1 DBD are expected to generate efficient competition against Ku for DNA ends and second because it offers a useful alternative to chemical inhibitors (30). We measured rejoining of DSBs in a cell line, COM3, conditionally expressing PARP-1 DBD under the control of a dexamethasone-inducible promoter (Supplementary Figure 2A). No changes in PARP-1 levels and no PARP-1 DBD expression are observed after treatment with dexamethasone in COR3 cells that only express the human glucocorticoid receptor (hGR). COM3 cells show detectable induction at 5 nM dexamethasone and steady further increase up to 500 nM, where expression reaches levels comparable to those of COC1 cells. Expression of PARP-1 DBD using 50 nM dexamethasone inhibits IR-induced PARP-1 activation, as measured by poly(ADP-ribose) analysis by western blotting (Supplementary Figure 2B), immunofluorescence (Supplementary Figure 2C) or the intracellular NAD^+ pools (Supplementary Figure 2D). Similar results

were obtained at higher concentrations of dexamethasone. Overexpression of PARP-1 DBD has been previously shown to inhibit DNA DSB rejoining in these cells (32). The results in Figure 1B demonstrate that under our conditions PARP-1 DBD expression causes a modest inhibition in DNA DSB rejoining, which is enhanced after inhibition of DNA–PK with wortmannin (Figure 1B). Wortmannin alone causes a strong delay in DSB rejoining (Figure 1B), although here again the majority of DSBs are removed by DNA–PK independent processes. The stronger effect of PARP-1 DBD expression on DSB rejoining, as compared to chemical inhibitors, on D-NHEJ deficient background suggests effects beyond PARP-1 inhibition and points to DNA-binding in competition with Ku.

PARP-1 contributes to the rejoining of plasmid DSBs in Ku or DNA ligase IV deficient cells

To further test the postulated competition between PARP-1 and Ku, we introduced an *in vivo* plasmid end joining assay. The assay allows, in addition to the generation of defined DSBs, also follow up of their repair in cells without other forms of DNA damage; IR exposed cells carry a 20-fold excess of SSBs and base damages compared to DSBs that compete for PARP-1. In this rapid-readout, direct-reporting plasmid assay, end joining is measured by the restitution of EGFP expression (21,44).

Principal characteristic of the plasmid (pEGFP-Pem1-Ad2) used in the assay (Figure 3A) is the interruption of the EGFP sequence by the Pem1 intron, within which restriction sites for HindIII and I-SceI are engineered upstream and downstream of the Ad2 exon (Figure 3A). Digestion with HindIII at both sites generates a linear plasmid with cohesive 5′-overhangs, whereas digestion with I-SceI at both sites and because of their inverted orientation, incompatible 3′-overhangs (Figure 3A). Because of the retention of the Ad2 exon, partial digestion at only one restriction site generates upon ligation a product unable to express EGFP. Due to the 'buffering' capacity of the intron, end joining of transfected, linearized plasmid by the cellular repair apparatus reconstitutes EGFP expression, even when extensive additions or deletions of nucleotides have occurred (44). As a result, a wide spectrum of end joining events can be detected.

When HindIII linearized plasmid is introduced into Ku proficient cells, intracellular circularization allowing EGFP expression is detected and quantitated by flow cytometry (Figure 3B). It is evident that plasmid rejoining in these cells is not affected by PARP-1 inhibitors (Figure 3B and C). In Ku80 deficient xrs-6 cells, on the other hand, the overall repair efficiency is lower. This may be a reflection of the reduced efficiency of B-NHEJ, the intracellular instability of the plasmid and the overall design of this experiment that preclude conclusions on ultimate end joining levels as is the case in experiments with genomic DNA (see Figures 1 and 2). However, residual end joining of HindIII linearized plasmid is reduced over 60% by 3′-AB or DIQ in Ku deficient cells, thus implicating PARP-1 in DSB rejoining under these conditions. A similar reduction in end joining is also observed in I-SceI linearized plasmid suggesting that the pathway rejoins both compatible as well as incompatible DNA ends (Figure 3B and C). A Chinese hamster mutant with defect in DNA–PKcs shows no reduction in DNA end joining after treatment either with 3′-AB or DIQ, suggesting a specific inhibitory effect for Ku on PARP-1 mediated end joining.

We carried out similar experiments using *LIG4*$^{-/-}$ and wild-type MEFs (6) to examine whether the small effect of PARP-1 inhibition observed in irradiated cells (Figure 1A) can be amplified in the plasmid assay that employs non-irradiated cells. Treatment of wild-type MEFs with 3′-AB or DIQ produces no effect on DNA end joining in HindIII digested plasmid (Figure 4A and B). In *LIG4*$^{-/-}$ MEFs, plasmid end joining is also observed, but in contrast to wild-type cells, treatment with 3′-AB or DIQ reduces end joining by over 60% (Figure 4A and B). A similar effect is observed with plasmid digested with I-SceI to generate incompatible ends. Thus, the plasmid assay detects a clear contribution of PARP-1 to DSB end joining when D-NHEJ is compromised by a defect in *LIG4*.

To examine whether Ku interferes with DNA end joining even under conditions where D-NHEJ is compromised by defects in proteins other than Ku, we knocked down Ku in *LIG4*$^{-/-}$ cells. With the selected (from three tested) siRNA sequence, western blotting shows a 70% knock-down effect (Figure 4D). Ku knock-down is accompanied by a nearly doubling in the efficiency of end joining in *LIG4*$^{-/-}$ MEFs (Figure 4C and D). Excess rejoining observed after Ku knock-down involves PARP-1, as it remains sensitive to 3′-AB (Figure 4E). Although here the relative effect of 3′-AB is similar to that of untreated controls, in absolute terms, a greater number of ends is prevented from joining after Ku knock-down due to the larger overall efficiency of the reaction (see Figure 4D). These results confirm a dominant negative effect of Ku in cells with defective D-NHEJ, and suggest that Ku binding limits the recruitment of alternative pathways utilizing PARP-1.

The observed difference in the magnitude of inhibition by 3′-AB or DIQ of IR-induced genomic DNA DSBs and of plasmid end joining in *LIG4*$^{-/-}$ cells can be attributed to competition for PARP-1 between DSBs and other DNA lesions present in great excess in irradiated cells. To examine this possibility, we treated *LIG4*$^{-/-}$ MEFs with H_2O_2 (5 mM, 5 min, RT) just before plasmid transfection to measure end joining and the effect of PARP-1 inhibitors (Figure 5). Untreated MEFs show the expected DNA end joining that is reduced by over 50% after treatment with either 3′-AB or DIQ (Figure 5A and B). Notably, inhibition of PARP-1 by the same inhibitors is less effective after treatment of cells with H_2O_2 suggesting a reduction in PARP-1 contribution, probably as a result of its engagement in the repair of H_2O_2 induced DNA SSB and base damages in genomic DNA. Reduced effect of PARP-1 inhibitors is seen despite an overall increase in DNA end joining capacity in H_2O_2 treated cells (Figure 5C). This increase probably reflects the redistribution of H_2O_2 treated cells throughout the cell cycle, and their accumulation in G2 (Figure 5C). Thus, the contribution of PARP-1 to DSB repair is compromised in the presence of H_2O_2 induced SSBs and base damages suggesting that in irradiated cells, the same lesions will divert PARP-1 from DSBs. In the absence of DNA ligase IV, DNA ligase III is expected to carry out the end joining required to generate the signal detected here. This suggests

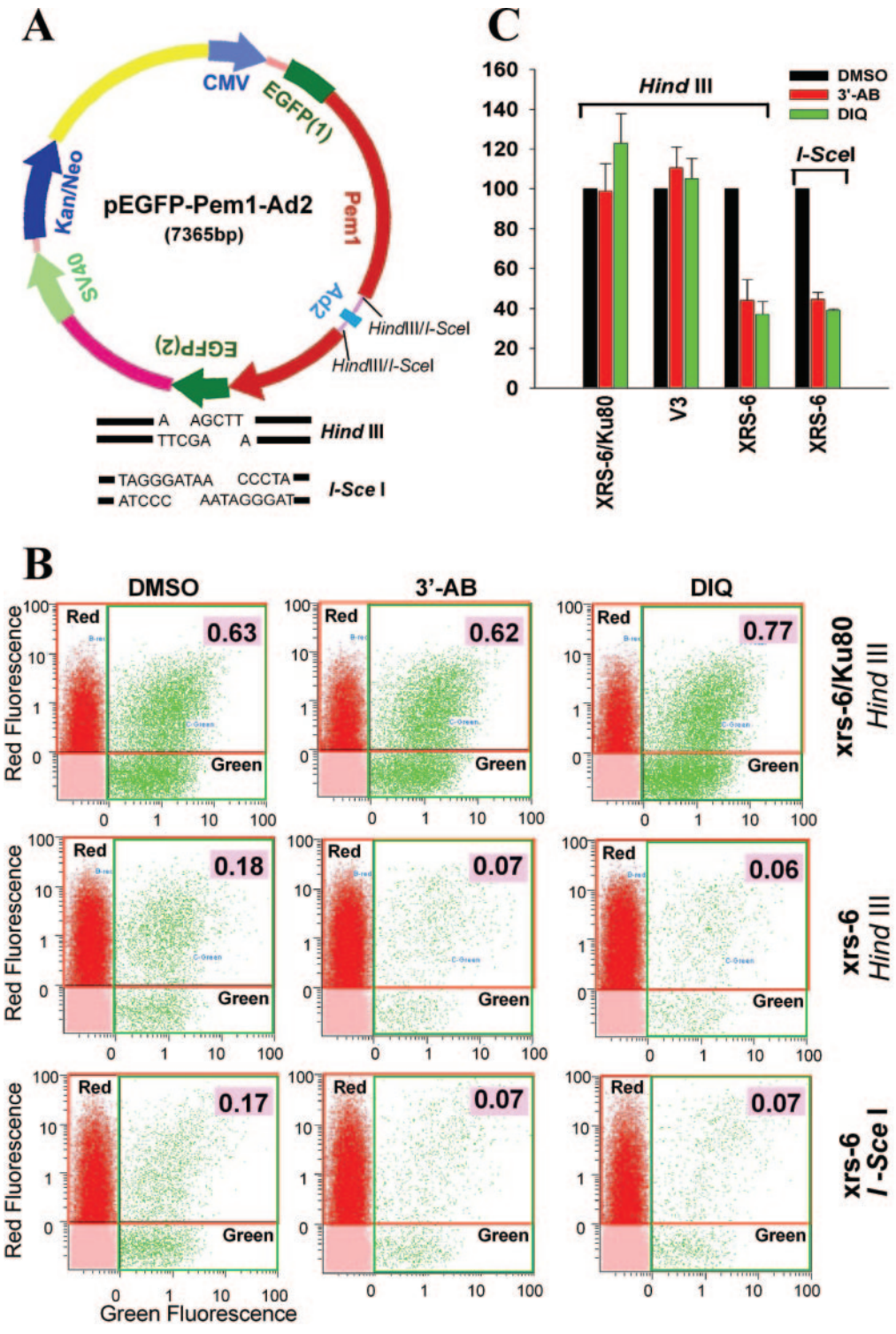

Figure 3. Effect of PARP-1 inhibitors on DNA end joining in Ku deficient cells using an *in vivo* plasmid assay. (**A**) Map of pEGFP-Pem1-Ad2 plasmid used. Note the HindIII and I-SceI restriction sites upstream and downstream the Ad2 exon that are used to linearize the plasmid and generate (after removal of Ad2) the ends shown in the lower part of the figure. Upon successful intracellular plasmid circularization EGFP expression is restored and quantitated by flow cytometry. (**B**) Two million cells were transfected with 200 ng of HindIII, or I-SceI linearized pEGFP-Pem1-Ad2 together with 200 ng supercoiled DsRed (to monitor transfection efficiency). The ratio of GFP^+ to $DsRed^+$ cells was calculated (values inserted in the individual dot plots) and used to determine the relative rejoining between samples exposed to inhibitors and samples left untreated. Results obtained with HindIII linearized plasmid in xrs6 and xrs-6/Ku80 cells, as well as with I-SceI linearized plasmid in xrs-6 cells are shown. Cells were pretreated with DMSO, 3′-AB (10 mM) and DIQ (100 μM) 1 h before electroporation and incubation with drugs continued in the 24 h allowed for repair and expression of the reporter genes. (**C**) Quantification of results shown in (B). Plotted is relative plasmid rejoining in xrs-6 and xrs-6/Ku80 cells treated with DMSO, 3′-AB or DIQ as calculated by dividing the $GFP^+/DsReD^+$ ratios of samples treated with inhibitors by those measured in cells treated with DMSO. Results obtained with cells transfected with HindIII, as well as I-SceI digested plasmid are shown. Included in the figure are also results obtained with the DNA–PKcs deficient mutant V3 (dot plots not shown).

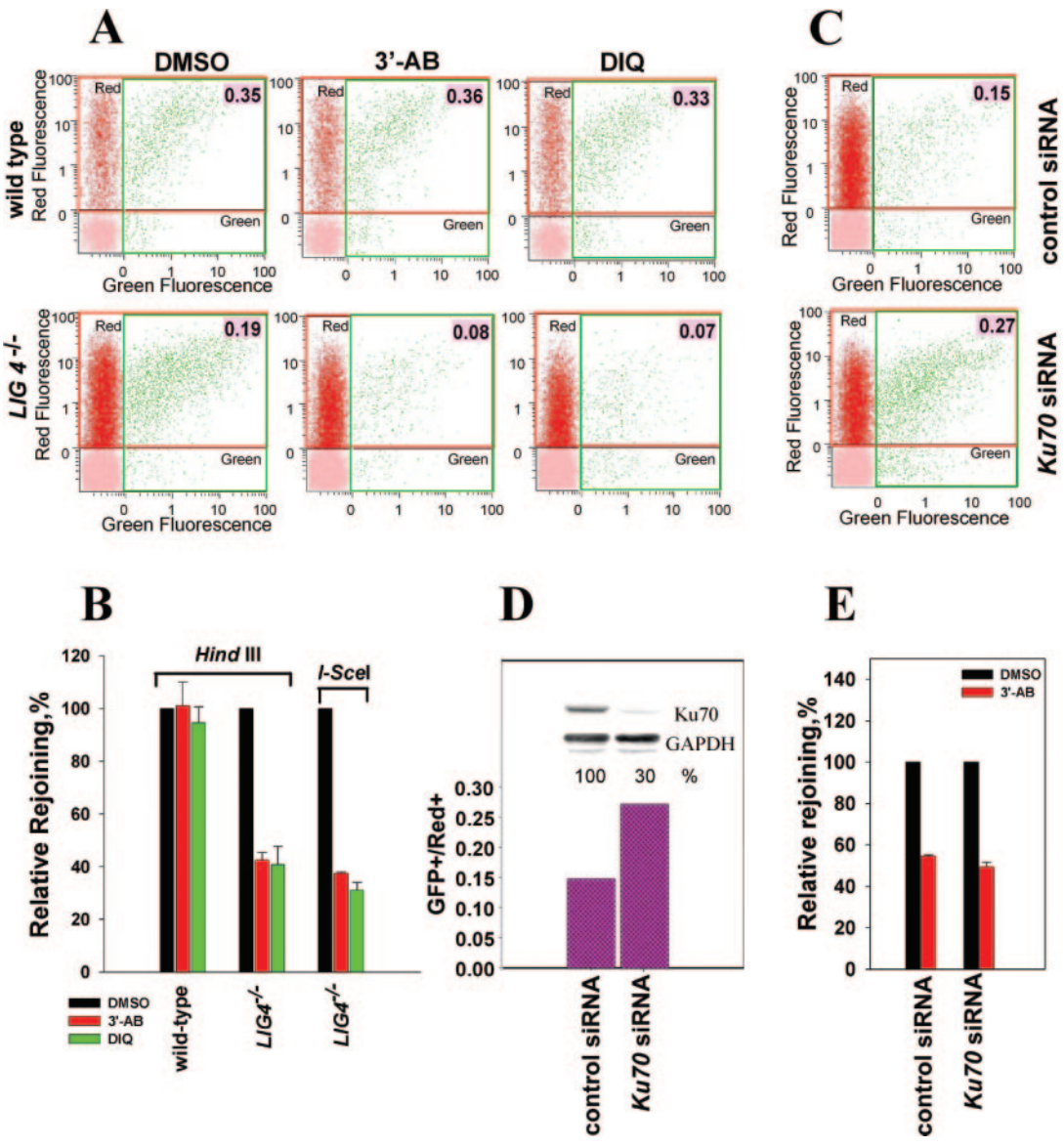

Figure 4. Effect of PARP-1 inhibitors on plasmid DNA end joining in LIG4$^{-/-}$ MEFs before and after Ku knock-down. (**A**) Flow cytometry dot plots showing the effect of 3′-AB and DIQ on rejoining of HindIII, or I-SceI, linearized pEGFP-Pem1-Ad2 in *p53*$^{-/-}$/*LIG4*$^{-/-}$ (200 ng plasmid), or *p53*$^{-/-}$ (wild-type) (50 ng plasmid) MEFs. Other details as in Figure 3. (**B**) Quantification of results shown in (A). Other details as in Figure 3. (**C**) Flow cytometry dot plots showing the effect of *KU70* knock-down on plasmid end joining in *p53*$^{-/-}$/*LIG4*$^{-/-}$ MEFs. The upper panel shows results of cells treated with control siRNA, while the lower panel results of cells treated with *KU70* siRNA. Other details as in Figure 3. (**D**) Quantification of results shown in (C). Plotted is the GFP^{+}/DsRed^{+} ratio for the two samples. The insert shows a western blot analyzing the level of knock-down at the time of plasmid transfection and shows Ku70 levels as well as the levels of GAPDH used as loading control. The percent knock-down achieved is also indicated. Plasmid was transfected 24 h after treatment with siRNA and flow cytometry was carried out after an additional incubation for 24 h. (**E**) Effect of 3′-AB on plasmid rejoining in *p53*$^{-/-}$/*LIG4*$^{-/-}$ MEFs treated with siRNA targeting *KU70*, as well as a control siRNA. Other details as in Figure 3.

that although PARP-1 participates in the reaction whenever available, it is not an absolute requirement for the reaction to take place.

Competition between PARP-1 and Ku for DNA end binding

We employed an EMSA to examine the DNA end binding properties of Ku and PARP-1 and to test competition between the two proteins for DNA ends. PARP-1 effectively binds a radioactively labeled double-stranded DNA substrate causing a mobility shift that is clearly detectable above 1 pmol protein (Supplementary Figure 3A). Because PARP-1 activity varies significantly depending on the type of DNA ends (49), we examined three substrates carrying 4 nt 3′ overhangs, blunt ends, or 1 nt 3′ overhangs. Since similar efficiency for DNA end binding is observed with all substrates, further experiments are carried out using 4 nt 3′ overhangs (OA/OB).

OA/OB binds also avidly to Ku (Supplementary Figure 3A), generating a measurable shift at 0.2 pmol and complete shift at 0.5 pmol protein. Thus, as expected (50) Ku binds DNA ends with an approximately 10-fold higher affinity than PARP-1. Because the band generated by Ku has an electrophoretic mobility very similar to that of PARP-1, a

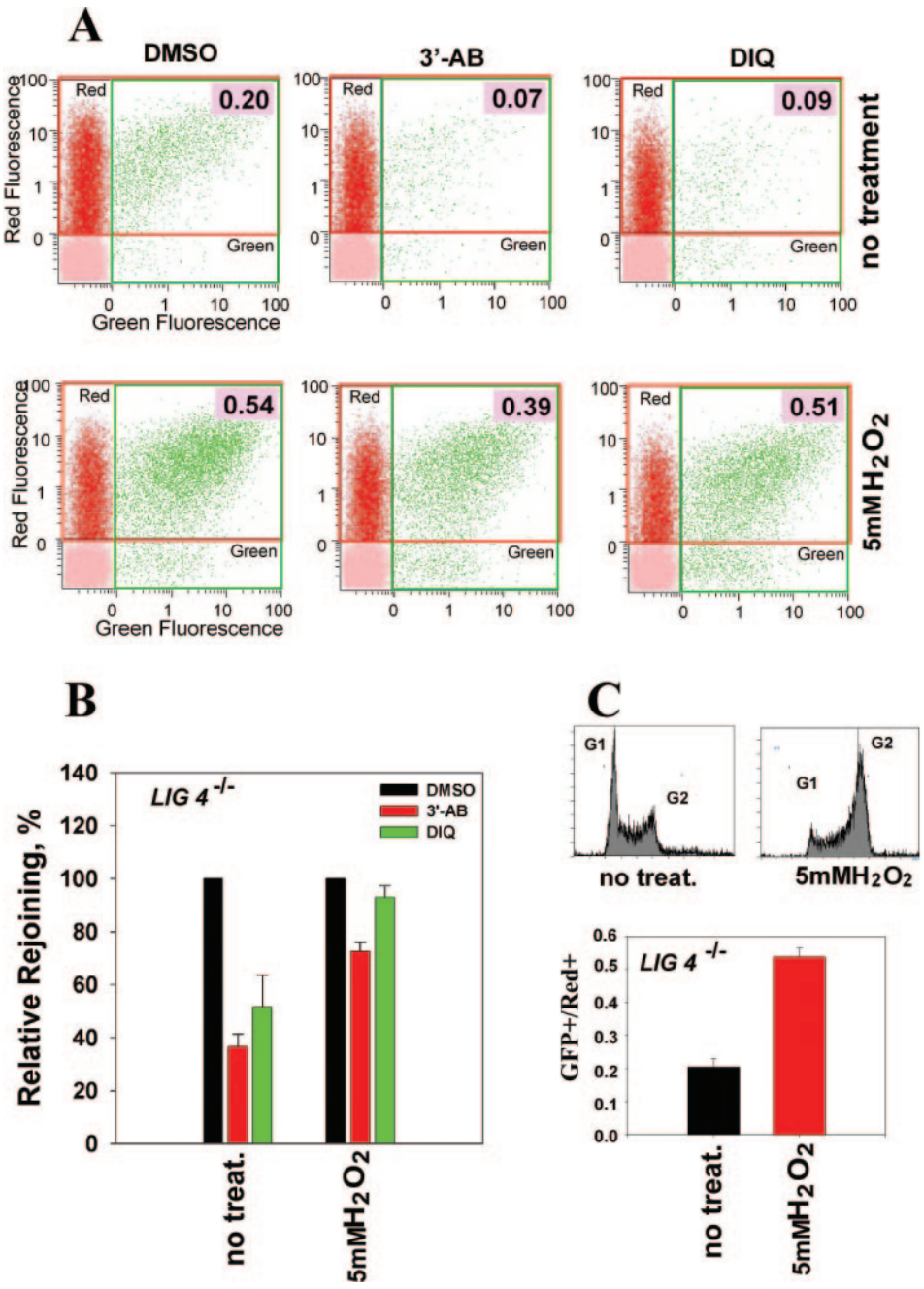

Figure 5. Effect of H_2O_2 treatment on plasmid DNA end joining in $p53^{-/-}$/LIG4$^{-/-}$ MEFs. (**A**) Flow cytometry dot plots showing $p53^{-/-}$/$LIG4^{-/-}$ MEFS treated for 5 min with 5 mM H_2O_2 at room temperature or left untreated, immediately transfected with 200 ng HindIII linearized pEGFP-Pem1-Ad2 and incubated for 24 h in the presence of DMSO, 3′-AB (10 mM) or DIQ (100 μM). DMSO treated cells were used as controls. Other details as in Figure 3. (**B**) Quantitative analysis of the results shown in (A). Data shown is normalized to that obtained in the absence of PARP-1 inhibitors. Other details as in Figure 3. (**C**) Plot of rejoining efficiency in untreated and H_2O_2 treated cells. The upper panel shows the cell cycle analysis of treated and non-treated cells at the time of analysis (24 h after transfection).

comparison of the DNA end binding characteristics in the presence of both proteins is not directly possible. We exploited antibody mediated supershift to separate Ku and PARP-1 bands. An anti-Ku80 antibody causes a robust supershift that clears the region of the original main Ku band allowing thus parallel analysis of PARP-1 DNA-binding (Supplementary Figure 3B). From the bands generated by supershift, the lower one (Ku-S1) is thought to reflect loading of each DNA end with a single Ku molecule, whereas the upper one (Ku-S2) loading with two Ku molecules (45). As expected, the mobility characteristics of PARP-1 are not affected by the anti-Ku antibody.

To examine competition between Ku and PARP-1, we first incubated substrate with Ku/antibody mixture and added subsequently PARP-1 at the indicated amounts (Figure 6). Ku at 0.2 pmol causes supershift for the majority of the substrate, mainly generating the band expected for single molecule loading (Figure 6A). Increasing amount of PARP-1 generates

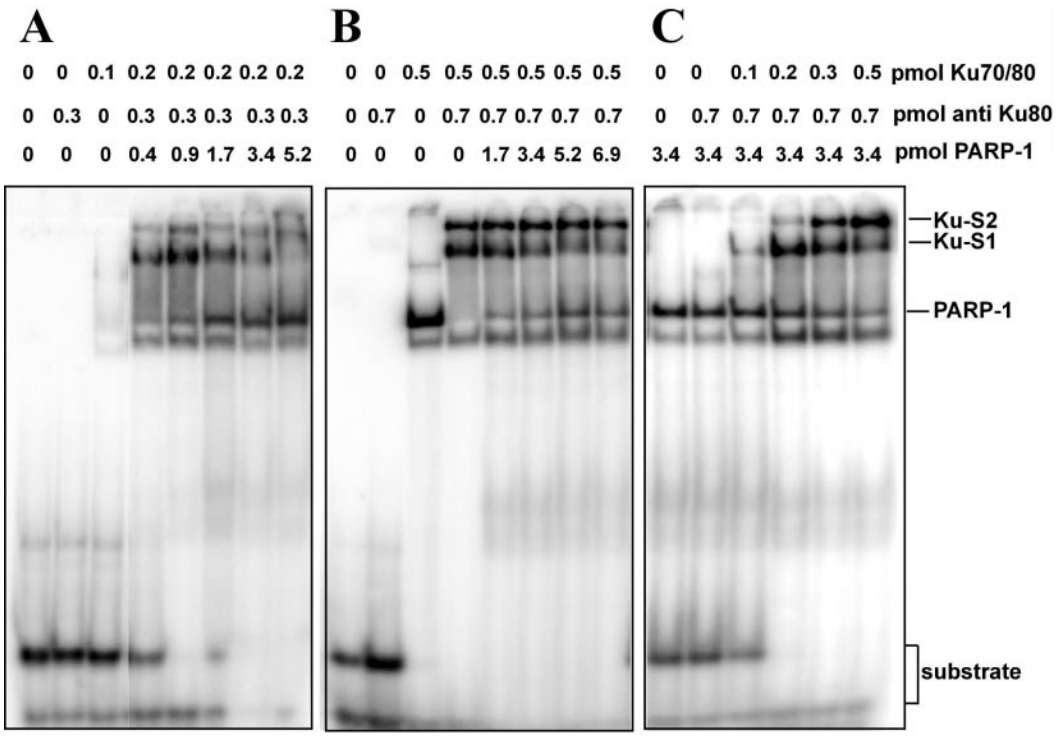

Figure 6. EMSA shows that Ku and PARP-1 compete for DNA ends. (**A**) EMSA was carried out by incubating the indicated amounts of Ku and anti-Ku80 antibody in the presence of 2 ng radioactively labeled OA/OB substrate for 15 min. Subsequently PARP-1 was added at the indicated amounts for 30 min, the reaction was stopped and products were analyzed by gel electrophoresis. Two bands generated by antibody mediated supershift of Ku are termed Ku-S1 and Ku-S2 and reflect loading of the substrate ends with one or two Ku molecules, respectively. The band generated by PARP-1 is also shown. (**B**) Same as A, but for reactions assembled with 0.5 pmol Ku and 0.7 pmol anti-Ku antibody. Note that Ku-S2 band gains intensity and that loaded Ku can be only partly displaced under these conditions. (**C**) Same as in A, but with reactions incubated first with 400 ng PARP-1 followed by incubation with the indicated amounts of KU and anti-KU antibody.

the expected band initially utilizing unbound substrate. At higher concentrations, however, the PARP-1 band is strengthened with parallel weakening of the Ku-S1 band (Figure 6A). Thus, PARP-1 displaces Ku from DNA ends, but a significant effect is observed at PARP-1/Ku molar ratios above ten. When the same assay is carried out with 0.5 pmol Ku (Figure 6B), two prominent bands are generated by supershift (Ku-S1 and Ku-S2), but PARP-1 effectively competes for DNA ends mainly populated by a single Ku molecule (Ku-S1). The greater stability of Ku-S2 band suggests that after loading of multiple Ku molecules, cooperative binding stabilizes the structure. When the same experiment is carried out in inverse sequence of protein addition, Ku effectively displaces PARP-1 from DNA ends, with more than two thirds removed after addition of 0.5 pmol protein (Figure 6C). These results are in line with previous observations in different model systems (51) and provide biochemical evidence for competition for DNA ends between PARP-1 and Ku, although successful displacement by PARP-1 requires concentrations higher by an order of magnitude than those of Ku. Such conditions may be approached after overexpression of PARP-1 DBD (Figure 1B and Supplementary Figure 2).

DISCUSSION

Taken together the results presented identify PARP-1 as a component of an alternative pathway of NHEJ and provide evidence that DNA end binding, in direct competition with Ku, is a key determinant of pathway selection. Additional data provide biochemical evidence for an engagement of DNA ligase III, a known partner of PARP-1, in DSB repair (21,22). In a directly relevant biochemical study using a novel two-step *in vitro* DNA end joining assay, immune to interference by Ku, Audebert *et al*. (22) reported that DNA end joining requires the synapsis activity of PARP-1 and the ligation activity of the XRCC1-DNA ligase III complex. Thus, the repair module PARP-1/DNA ligase III/XRCC1 (PLX), hitherto regarded as central in SSB repair (52,53), is implicated in the repair of DSBs. This function may not rely on novel activities, as DSBs form when SSBs occur in close proximity, in opposite DNA strands. The much higher affinity of Ku for DNA ends will limit the contribution of this form of end joining to instances where the classical pathway is compromised. As a result, its function will be more that of a backup (B-NHEJ) and less of an 'alternative' repair pathway (54).

Several reports implicate inferior backup pathways of DNA end joining in the phenotypes of mutants of the classical NHEJ pathway. Thus, non-classical pathways of end joining bring together the *c-myc* and *Igh* locus and cause B-cell lymphomas in mice with defects in *Ku*, *LIG4* or *XRCC4* (5–8,11,12,55). Functionally equivalent pathways may generate the aberrant junctions manifesting chromosome instability in the same mutants. Non-classical pathways of end joining generate the few V(D)J junctions observed in cells with

defects in NHEJ (14,15,17) and are implicated in antibody class switching occurring under the same conditions (55). Although not formally demonstrated, PARP-1 may be participating in these forms of non-classical end joining [e.g. (56)]. Furthermore, the substantial DNA end joining observed after exposure to IR of cells with defects in DNA ligase IV, Ku and DNA–PK (Figures 1 and 2, and Supplementary Figure 1) directly implicates alternative forms of DNA end joining. The results presented here and published data (21,22) implicate PARP-1 and DNA Ligase III in this function.

PARP-1/DNA Ligase III dependent end joining, when utilized, helps the cell to restore its genome and thus presumably to avert cell death. However, its error prone nature causes genomic instability and cancer in the affected organism. The adverse consequences of this repair pathway may derive from inefficient synapsis of the DNA ends, which is probably supported only by microhomologies (9,10) and is therefore inefficient and slow [Figures 1 and 2, and Supplementary Figure 1; and (19,54,57)]. The resulting persistence of DNA ends in the cell can lead to incorrect rejoining and thus to translocations. In addition, it may facilitate DNA end degradation and thus loss of genetic information. Both phenomena have been described in mutants of the classical pathway of DNA end joining (see above).

While prominent when the classical pathway is compromised, the backup pathway may theoretically be utilized to a limited degree in cells with functional D-NHEJ as well. This can occur when a DSB is induced in a nuclear region where Ku or other key components of D-NHEJ, are not immediately available; for example because they are already recruited to a neighboring DSB. Such contributions may underlie micronuclei observed in *PARP-1*$^{-/-}$ cells (58), as well as genomic instability and occasionally tumor development in *PARP-1*$^{-/-}$ mice on *p53*$^{-/-}$ background (59,60).

Our results further show that the function of PARP-1 in DSB repair will be competed by its canonical function in SSB repair. Reduced engagement in the repair of a highly dangerous lesion as the DSB through competition by a less severe one, a SSB, is a limitation of the pathway and justifies its ranking as a backup. It follows that DSBs induced by agents generating higher ratios of DSBs to SSBs than IR, e.g. calicheamicin γ^{I}, are more likely to engage PARP-1 (22). However, this distinction of severity between SSBs and DSBs may be altered during S phase, where SSBs can be converted to one-ended DSBs which, if not repaired by HRR, can have serious consequences for the cell (28,29).

Inhibition of a PARP-1 dependent backup pathway of DSB end joining partly explains the lethality of *PARP-1*$^{-/-}$/*Ku*$^{-/-}$ mice (61), as normal development may not be compatible with inactivation of both NHEJ pathways. Along similar lines it can be reasoned that the lethality of *PARP-1*$^{-/-}$/*ATM*$^{-/-}$ mice partly derives from a contribution of ATM to a subset of radiation-induced complex DSBs that require D-NHEJ (62). Also, tumor formation in *PARP-1*$^{-/-}$ mice engineered with Ku haploinsufficiency (63), or DNA–PK knock out (64), suggests that reduction in the efficiency of D-NHEJ favors PARP-1 dependent end joining and thus genomic instability and cancer. Finally, the rescue of *LIG4*$^{-/-}$ lethality and radiosensitivity by *Ku* knock out (65,66) can be explained by the relief of the dominant negative inhibition exerted by Ku on backup end joining in *LIG4*$^{-/-}$ cells. However, the recent observation that PARP-1 protects HRR from interference by KU and DNA Ligase IV (67) also suggests that KU-mediated down regulation of HRR may partly underlie the above described phenomena. Finally, it is also possible that defects in SSB repair resulting from PARP-1 deficiency contribute to the described effects. More work is needed to discriminate between these possible contributions.

The biochemical properties of PARP-1 are compatible with its function in a backup pathway of NHEJ. PARP-1 binds and becomes activated by double-stranded DNA ends (49,68), even during V(D)J recombination (56), as it would be anticipated by a protein involved in DSB repair. The affinity of PARP-1 for DNA ends generates an activity analogous to Ku and offers an alternative mode of recognition of this type of lesion. Although PARP-1 has been repeatedly implicated in DSB repair, divergent results have hampered the formulation of a consistent model (34,69). Our observations, as well as those published earlier (22), implicate this activity in a backup rather in the canonical pathway of end joining and provide a new dimension for re-evaluating these experiments.

Although inhibition of PARP-1 compromises DSB rejoining both in the plasmid assay as well as in irradiated cells, the inhibition is never complete and actually rather limited for DSBs induced in genomic DNA (Figures 1 and 2). This suggests that rejoining of DSBs remains possible in the absence of PARP-1 and may be carried out by DNA ligase III, possibly aided by its zinc finger domain (21,22).

The hierarchical organization of the classical and backup pathways of end joining may be regulated by interactions between the participating proteins. Thus, DNA–PKcs is poly(ADP-ribosyl)ated *in vitro* by PARP-1 and this modification stimulates DNA–PK activity (70). On the other hand, DNA–PK suppresses PARP-1 activity but probably not through the associated phosphorylation (50). Similarly, the BRCT1 domain of XRCC1 is phosphorylated by DNA–PK and this phosphorylation causes XRCC1 dimer dissociation (71). At the same time, interaction between XRCC1 and DNA–PK stimulates the kinase activity towards p53 (71). It is notable that all these inputs further consolidate the hierarchical organization of end joining by favoring the engagement of the classical pathway and suppressing the utilization of the backup pathway.

Our results in aggregate implicate PARP-1 in DSB repair through participation in a backup pathway together with DNA Ligase III and possibly XRCC1. This function is enabled by the considerable affinity of PARP-1 for double-stranded DNA ends, is under normal conditions competed by Ku and may further be down-regulated by DNA–PK. Additional modulation of engagement for DSB repair is afforded by PARP-1 recruitment to SSB. Our experiments focus on PARP-1. However among the eighteen potential PARPs in the mammalian genome, PARP-2 has also been implicated in repair functions equivalent to those of PARP-1 (24). It remains to be seen whether PARP-2 can also contribute to backup end joining of DSBs as suggested here for PARP-1.

SUPPLEMENTARY DATA

Supplementary Data are available at NAR Online.

ACKNOWLEDGEMENTS

The authors are indebted to Prof. Dr Alexander Brückle for reagents and advice, as well as to Joan Allalunis-Turner, Fed Alt, David Chen, Penny Jeggo, Gloria Li and Klaus Weber for cell lines. Special thanks go to Vera Gorbunova for providing pEGFP-Pem1-Ad2 and to Lei Li for pEGFP-Pem1. This work was partly supported by a grant from the DFG. Funding to pay the Open Access publication charges for this article was provided by DFG.

Conflict of interest statement. None declared.

REFERENCES

1. Khanna,K.K. and Jackson,S.P. (2001) DNA double-strand breaks: signaling, repair and the cancer connection. *Nature Genet*., **27**, 247–254.
2. Sancar,A., Lindsey-Boltz,L.A., Ünsal-Kacmaz,K. and Linn,S. (2004) Molecular mechanisms of mammalian DNA repair and the DNA damage checkpoints. *Annu. Rev. Biochem*., **73**, 39–85.
3. Ahnesorg,P., Smith,P. and Jackson,S.P. (2006) XLF interacts with the XRCC4-DNA ligase IV complex to promote DNA nonhomologous end-joining. *Cell*, **124**, 301–313.
4. Buck,D., Malivert,L., de Chasseval,R., Barraud,A., Fondaneche,M.-C., Sanal,O., Plebani,A., Stephan,J.-L., Hufnagel,M. and le Deist,F. (2006) Cernunnos, a novel nonhomologous end-joining factor, is mutated in human immunodeficiency with microcephaly. *Cell*, **124**, 287–299.
5. Difilippantonio,M.J., Zhu,J., Chen,H.T., Meffre,E., Nussenzweig,N.C., Max,E.E., Ried,T. and Nussenzweig,A. (2000) DNA repair protein Ku80 suppresses chromosomal aberrations and malignant transformation. *Nature*, **404**, 510–514.
6. Frank,K.M., Sharpless,N.E., Gao,Y., Sekiguchi,J.M., Fergson,D.O., Zhu,C., Manis,J.P., Horner,J., DePinho,R.A. and Alt,F.W. (2000) DNA ligase IV deficiency in mice leads to defective neurogenesis and embryonic lethality via the p53 pathway. *Mol. Cell*, **5**, 993–1002.
7. Gao,Y., Ferguson,D.O., Xie,W., Manis,J.P., Sekiguchi,J.A., Frank,K.M., Chaudhuri,J., Horner,J., DePinho,R.A. and Alt,F.W. (2000) Interplay of p53 and DNA-repair protein XRCC4 in tumorigenesis, genomic stability and development. *Nature*, **404**, 897–900.
8. Zhu,C., Mills,K.D., Ferguson,D.O., Lee,C., Manis,J., Fleming,J., Gao,Y., Morton,C.C. and Alt,F.W. (2002) Unrepaired DNA breaks in p53-deficient cells lead to oncogenic gene amplification subsequent to translocations. *Cell*, **109**, 811–821.
9. Verkaik,N.S., Esveldt-van Lange,R.E.E., van Heemst,D., Brüggenwirth,H.T., Hoeijmakers,J.H.J., Zdzienicka,M.Z. and van Gent,D.C. (2002) Different types of V(D)J recombination and end-joining defects in DNA double-strand break repair mutant mammalian cells. *Eur. J. Immunol*., **32**, 701–709.
10. Roth,D.B. and Wilson,J.H. (1986) Nonhomologous recombination in mammalian cells: role for short sequence homologies in the joining reaction. *Mol. Cell. Biol*., **6**, 4295–4304.
11. Karanjawala,Z.E., Grawunder,U., Hsieh,C.-L. and Lieber,M.R. (1999) The nonhomologous DNA end joining pathway is important for chromosome stability in primary fibroblasts. *Curr. Biol*., **9**, 1501–1504.
12. Ferguson,D.O., Sekiguchi,J.M., Chang,S., Frank,K.M., Gao,Y., DePinho,R.A. and Alt,F.W. (2000) The nonhomologous end-joining pathway of DNA repair is required for genomic stability and the suppression of translocations. *Proc. Natl Acad. Sci. USA*, **97**, 6630–6633.
13. Sharpless,N.E., Ferguson,D.O., O'Hagan,R.C., Castrillon,D.H., Lee,C., Farazi,P.A., Alson,S., Fleming,J., Morton,C.C., Frank,K. *et al*. (2001) Impaired nonhomologous end-joining provokes soft tissue sarcomas harboring chromosomal translocations, amplifications, and deletions. *Mol. Cell*, **8**, 1187–1196.
14. Bogue,M.A., Wang,C., Zhu,C. and Roth,D.B. (1997) V(D)J Recombination in Ku86-deficient mice: Distinct effects on coding, signal, and hybrid joint formation. *Immunity*, **7**, 37–47.
15. Li,Z., Otevrel,T., Gao,Y., Cheng,W.-L., Seed,B., Stamato,T.D., Taccioli,G.E. and Alt,F.W. (1995) The XRCC4 gene encodes a novel protein involved in DNA double-strand break repair and V(D)J recombination. *Cell*, **83**, 1079–1089.
16. Taccioli,G.E., Rathbun,G., Oltz,E., Stamato,T., Jeggo,P.A. and Alt,F.W. (1993) Impairment of V(D)J recombination in double-strand break repair mutants. *Science*, **260**, 207–210.
17. Lee,G.S., Neiditch,M.B., Salus,S.S. and Roth,D.B. (2004) RAG proteins shepherd double-strand breaks to a specific pathway, suppressing error-prone repair, but RAG nicking initiates homologous recombination. *Cell*, **117**, 171–184.
18. Nevaldine,B., Longo,J.A. and Hahn,P.J. (1997) The *scid* defect results in much slower repair of DNA double-strand breaks but not high levels of residual breaks. *Radiat. Res*., **147**, 535–540.
19. DiBiase,S.J., Zeng,Z.-C., Chen,R., Hyslop,T., Curran,W.J.,Jr and Iliakis,G. (2000) DNA-dependent protein kinase stimulates an independently active, nonhomologous, end-joining apparatus. *Cancer Res*., **60**, 1245–1253.
20. Wang,H., Zeng,Z.-C., Bui,T.-A., Sonoda,E., Takata,M., Takeda,S. and Iliakis,G. (2001) Efficient rejoining of radiation-induced DNA double-strand breaks in vertebrate cells deficient in genes of the RAD52 epistasis group. *Oncogene*, **20**, 2212–2224.
21. Wang,H., Rosidi,B., Perrault,R., Wang,M., Zhang,L., Windhofer,F. and Iliakis,G. (2005) DNA ligase III as a candidate component of backup pathways of nonhomologous end joining. *Cancer Res*., **65**, 4020–4030.
22. Audebert,M., Salles,B. and Calsou,P. (2004) Involvement of poly(ADP-ribose) polymerase-1 and XRCC1/DNA ligase III in an alternative route for DNA double-strand breaks rejoining. *J. Biol. Chem*., **279**, 55117–55126.
23. D'Amours,D., Desnoyers,S., D'Silva,I. and Poirier,G.G. (1999) Poly(ADP-ribosyl)ation reactions in the regulation of nuclear functions. *Biochem. J*., **342**, 249–268.
24. Ame,J.-C., Spenlehauer,C. and de Murcia,G. (2004) The PARP superfamily. *BioEssays*, **26**, 882–893.
25. Kim,M.Y., Zhang,T. and Kraus,W.L. (2005) Poly(ADP-ribosyl)ation by PARP-1: 'PAR-laying' NAD+ into a nuclear signal. *Genes Dev*., **19**, 1951–1967.
26. Okano,S., Lan,L., Caldecott,K.W., Mori,T. and Yasui,A. (2003) Spatial and temporal cellular responses to single-strand breaks in human cells. *Mol. Cell. Biol*., **23**, 3974–3981.
27. Frouin,I., Maga,G., Denegri,M., Riva,F., Savio,M., Spadari,S., Prosperi,E. and Scovassi,I. (2003) Human proliferating cell nuclear antigen, poly(ADP-ribose) polymerase-1, and $p21^{waf1/cip1}$. *J. Biol. Chem*., **278**, 39265–39268.
28. Farmer,H., McCabe,N., Lord,C.J., Tutt,A.N.J., Johnson,D.A., Richardson,T.B., Santarosa,M., Dillon,K.J., Hickson,I., Knights,C. *et al*. (2005) Targeting the DNA repair defect in BRCA mutant cells as a therapeutic strategy. *Nature*, **434**, 917–921.
29. Bryant,H.E., Schultz,N., Thomas,H.D., Parker,K.M., Flower,D., Lopez,E., Kyle,S., Meuth,M., Curtin,N.J. and Helleday,T. (2005) Specific killing of BRCA2-deficient tumours with inhibitors of poly(ADP-ribose) polymerase. *Nature*, **434**, 913–917.
30. Küpper,J.H., Müller,M., Jacobson,M.K., Tatsumi-Miyajima,J., Coyle,D.L., Jacobson,E.L. and Bürkle,A. (1995) *trans*-Dominant inhibition of poly(ADP-Ribosyl)ation sensitizes cells against γ−irradiation and N-methyl-N′-nitrosoguanidine but does not limit DNA replication of a polyomavirus peplicon. *Mol. Cell. Biol*., **15**, 3154–3163.
31. Tatsumi-Miyajima,J., Küpper,J.-H., Takebe,H. and Bürkle,A. (1999) *trans-Dominant* inhibition of poly (ADP-ribosyl)ation potentiates alkylation-induced shuttle-vector mutagenesis in Chinese hamster cells. *Mol. Cell. Biochem*., **193**, 31–35.
32. Rudat,V., Bachmann,N., Küpper,J.-H. and Weber,K.-J. (2001) Overexpression of the DNA-binding domain of poly(ADP-ribose) polymerase inhibits rejoining of ionizing radiation-induced DNA double-strand breaks. *Int. J. Radiat. Biol*., **77**, 303–307.
33. Süsse,S., Scholz,C.-J., Bürkle,A. and Wiesmüller,L. (2004) Poly(ADP-ribose) polymerase (PARP-1) and p53 independently function in regulating double-strand break repair in primate cells. *Nucleic Acids Res*., **32**, 669–680.
34. Noel,G., Giocanti,N., Fernet,M., Megnin-Chanet,F. and Favaudon,V. (2003) Poly(ADP-ribose) polymerase (PARP-I) is not involved in DNA double-strand break recovery. *BMC Cell. Biol*., **4**, 7–16.

35. Yang,Y.-G., Cortes,U., Patnaik,S., Jasin,M. and Wang,Z.-Q. (2004) Ablation of PARP-1 does not interfere with the repair of DNA double-strand breaks, but compromises the reactivation of stalled replication forks. *Oncogene*, **23**, 3872–3882.
36. Lees-Miller,S.P., Godbout,R., Chan,D.W., Weinfeld,M., Day,R.S., III, Barron,G.M. and Allalunis-Turner,J. (1995) Absence of p350 subunit of DNA-activated protein kinase from a radiosensitive human cell line. *Science*, **267**, 1183–1185.
37. Ouyang,B.H., Nussenzweig,A., Kurimasa,A., da Costa Soares,V., Li,X., Cordon-Cardo,C., Li,W.-h., Cheong,N., Nussenzweig,M., Iliakis,G. *et al*. (1997) Ku70 is required for DNA repair but not for T cell antigen receptor gene recombination *in vivo*. *J. Exp. Med*., **186**, 921–929.
38. Ross,G.M., Eady,J.J., Mithal,N.P., Bush,C., Steel,G.G., Jeggo,P.A. and McMillan,T.J. (1995) DNA strand break rejoining defect in *xrs-6* is complemented by transfection with the human *Ku80* gene. *Cancer Res*., **55**, 1235–1238.
39. Jacobson,E.L., Jacobson,M.K. and Bernofsky,C. (1974) NAD Levels in 3T3 Cells during exponential growth and density-dependent inhibition of growth. *FEBS Lett*., **47**, 23–25.
40. Jacobson,E.L. and Jacobson,M.K. (1976) Pyridine nucleotide levels as a function of growth in normal and transformed 3T3 Cells. *Arch. Biochem. Biophys*., **175**, 627–634.
41. Yoo,S., Kimzey,A. and Dynan,W.S. (1999) Photocross-linking of an oriented DNA repair complex. *J. Biol. Chem*., **274**, 20034–20039.
42. Iliakis,G., Metzger,L., Denko,N. and Stamato,T.D. (1991) Detection of DNA double strand breaks in synchronous cultures of CHO cells by means of asymmetric field inversion gel electrophoresis. *Int. J. Radiat. Biol*., **59**, 321–341.
43. Stenerlöw,B., Karlsson,K.H., Cooper,B. and Rydberg,B. (2003) Measurement of prompt DNA double-strand breaks in mammalian cells without including heat-labile sites: results for cells deficient in nonhomologous end joining. *Radiat. Res*., **159**, 502–510.
44. Seluanov,A., Mittelman,D., Pereira-Smith,O.M., Wilson,J.H. and Gorbunova,V. (2004) DNA end joining becomes less efficient and more error-prone during cellular senescence. *Proc. Natl Acad. Sci. USA*, **101**, 7624–7629.
45. Hammarsten,O. and Chu,G. (1998) DNA-dependent protein kinase: DNA binding and activation in the absence of Ku. *Proc. Natl Acad. Sci. USA*, **95**, 525–530.
46. Wang,H., Perrault,A.R., Takeda,Y., Qin,W., Wang,H. and Iliakis,G. (2003) Biochemical evidence for Ku-independent backup pathways of NHEJ. *Nucleic Acids Res*., **31**, 5377–5388.
47. Anderson,C.W., Dunn,J.J., Freimuth,P.I., Galloway,A.M. and Allalunis-Turner,M.J. (2001) Frameshift mutation in PRKDC, the gene for DNA–PKcs, in the DNA repair-defective, human, glioma-derived cell line M059J. *Radiat. Res*., **156**, 2–9.
48. Molinete,M., Vermeulen,W., Burkle,A., Menissier-de Murcia,J., Kupper,J., Hoeijmakers,J. and de Murcia,G. (1993) Overproduction of the poly(ADP-ribose) polymerase DNA-binding domain blocks alkylation-induced DNA repair synthesis in mammalian cells. *EMBO J*., **12**, 2109–2117.
49. D'Silva,I., Pelletier,J.D., Lagueux,J., D'Amours,D., Chaudhry,M.A., Weinfeld,M., Lees-Miller,S.P. and Poirier,G.G. (1999) Relative affinities of poly(ADP-ribose) polymerase and DNA-dependent protein kinase for DNA strand interruptions. *Biochim. Biophys. Acta*, **1430**, 119–126.
50. Ariumi,Y., Masutani,M., Copeland,T.D., Mimori,T., Sugimura,T., Shimotohno,K., Ueda,K., Hatanaka,M. and Noda,M. (1999) Suppression of the poly (ADP-ribose) polymerase activity by DNA-dependent protein kinase *in vitro*. *Oncogene*, **18**, 4616–4625.
51. Galande,S. and Kohwi-Shigematsu,T. (1999) Poly(ADP-ribose) polymerase and Ku autoantigen form a complex and synergistically bind to matrix attachment sequences. *J. Biol. Chem*., **274**, 20521–20528.
52. Caldecott,K.W. (2001) Mammalian DNA single-strand break repair: an X-ra(y)ted affair. *Bioessays*, **23**, 447–455.
53. Tomkinson,A. and Levin,D.S. (1997) Mammalian DNA ligases. *Bioessays*, **19**, 893–901.
54. Iliakis,G., Wang,H., Perrault,A.R., Boecker,W., Rosidi,B., Windhofer,F., Wu,W., Guan,J., Terzoudi,G. and Pantelias,G. (2004) Mechanisms of DNA double strand break repair and chromosome aberration formation. *Cytogenet. Genome Res*., **104**, 14–20.
55. Ramiro,A.R., Jankovic,M., Callen,E., Difilippantonio,S., Chen,H.-T., McBride,K.M., Eisenreich,T.R., Chen,J., Dickins,R.A., Lowe,S.W. *et al*. (2006) Role of genomic instability and p53 in AID-induced c-myc-Igh translocations. *Nature*, **440**, 105–109.
56. Brown,M.L., Franco,D., Bürkle,A. and Chang,Y. (2002) Role of poly(ADP-ribosyl)ation in DNA–PK_{cs}-independent V (D)J recombination. *Proc. Natl Acad. Sci. USA*, **99**, 4532–4537.
57. Wang,H., Zhao-Chong,Z., Perrault,A.R., Cheng,X., Qin,W. and Iliakis,G. (2001) Genetic evidence for the involvement of DNA ligase IV in the DNA–PK-dependent pathway of non-homologous end joining in mammalian cells. *Nucleic Acids Res*., **29**, 1653–1660.
58. Wang,Z.-Q., Stingl,L., Morrison,C., Jantsch,M., Los,M., Schulze-Osthoff,K. and Wagner,E.F. (1997) PARP is important for genomic stability but dispensable in apoptosis. *Genes Dev*., **11**, 2347–2358.
59. Tong,W.-M., Hande,M.P., Lansdorp,P.M. and Wang,Z.-Q. (2001) DNA Strand break-sensing molecule poly(ADP-Ribose) polymerase cooperates with p53 in telomere function, chromosome stability, and tumor suppression. *Mol. Cell. Biol*., **21**, 4046–4054.
60. Conde,C., Mark,M., Oliver,F.J., Huber,A., De Murcia,G. and Menissier-de Murcia,J. (2001) Loss of poly(ADP-ribose) polymerase-1 causes increased tumour latency in p53-deficient mice. *EMBO J*., **20**, 3535–3543.
61. Henrie,M.S., Kurimasa,A., Burma,S., Menissier de Murcia,J., de Murcia,G., Li,G.C. and Chen,D.J. (2003) Lethality in PARP-1/Ku80 double mutant mice reveals physiological synergy during early embryogenesis. *DNA Repair (Amst.)*, **2**, 151–158.
62. Riballo,E., Kühne,M., Rief,N., Doherty,A., Smith,G.C.M., Recio,M.-J., Reis,C., Dahm,K., Fricke,A., Krempler,A. *et al*. (2004) A pathway of double-strand break rejoining dependent upon ATM, artemis, and proteins locating to γ-H2AX Foci. *Mol. Cell*, **16**, 715–724.
63. Tong,W.-M., Cortes,U., Hande,M.P., Ohgaki,H., Cavalli,L.R., Lansdorp,P.M., Haddad,B.R. and Wang,Z.-Q. (2002) Synergistic role of Ku80 and poly(ADP-ribose) polymerase in suppressing chromosomal aberrations and liver cancer formation. *Cancer Res*., **62**, 6990–6996.
64. Morrison,C., Smith,G.C.M., Stingl,L., Jackson,S.P., Wagner,E.F. and Wang,Z.-Q. (1997) Genetic interaction between PARP and DNA–PK in V(D)J recombination and tumorigenesis. *Nature Genet*., **17**, 479–482.
65. Karanjawala,Z.E., Adachi,N., Irvine,R.A., Oh,E.K., Shibata,D., Schwarz,K., Hsieh,C.-L. and Lieber,M.R. (2002) The embryonic lethality in DNA ligase IV-deficient mice is rescued by deletion of Ku: implications for unifying the heterogeneous phenotypes of NHEJ mutants. *DNA Repair (Amst.)*, **1**, 1017–1026.
66. Adachi,N., Ishino,T., Ishii,Y., Takeda,S. and Koyama,H. (2001) DNA ligase IV-deficient cells are more resistant to ionizing radiation in the absence of Ku70: implications for DNA double-strand break repair. *Proc. Natl Acad. Sci. USA*, **98**, 12109–12113.
67. Hochegger,H., Dejsuphong,D., Fukushima,T., Morrison,C., Sonoda,E., Schreiber,V., Zhao,G.Y., Saberi,A., Masutani,M., Adachi,N. *et al*. (2006) Parp-1 protects homologous recombination from interference by Ku and ligase IV in vertebrate cells. *EMBO J*., **25**, 1305–1314.
68. Kun,E., Kirsten,E. and Ordahl,C.P. (2002) Coenzymatic activity of randomly broken or intact double-stranded DNAs in auto and histone H_1 trans-poly(ADP-ribosylation), catalyzed by poly(ADP-ribose) polymerase (PARP I). *J. Biol. Chem*., **277**, 39066–39069.
69. Veuger,S.J., Curtin,N.J., Smith,G.C.M. and Durkacz,B.W. (2004) Effects of novel inhibitors of poly(ADP-ribose) polymerase-1 and the DNA-dependent protein kinase on enzyme activities and DNA repair. *Oncogene*, **23**, 7322–7329.
70. Ruscetti,T., Lehnert,B.E., Halbrook,J., Trong,H.L., Hoekstra,M.F., Chen,D.J. and Peterson,S.R. (1998) Stimulation of the DNA-dependent protein kinase by poly(ADP-ribose) polymerase. *J. Biol. Chem*., **273**, 14461–14467.
71. Levy,N., Martz,A., Bresson,A., Spenlehauer,C., De Murcia,G. and Menissier-de Murcia,J. (2006) XRCC1 is phosphorylated by DNA-dependent protein kinase in response to DNA damage. *Nucleic Acids Res*., **34**, 32–41.